Research Square

Preprints are preliminary reports that have not undergone peer review.
They should not be considered conclusive, used to inform clinical practice,
or referenced by the media as validated information.

Flexural Fatigue Performance Analysis of Bridge T-Beam Members Strengthened with Prestressed CFRP Plates

Qiang Lu
School of Civil Engineering, Chongqing Vocational Institute of Engineering
Fengbing Zhao
zhao.fengbing@163.com
School of Civil Engineering, Guizhou University of Engineering Science
Bolin Jiang
School of Civil Engineering, Chongqing Vocational Institute of Engineering
Shanshan Wu
School of Railways and Architecture, Chongqing Vocational College of Public Transportation

Article

Keywords: Prestressed CFRP plates, girder bridges, flexural fatigue, structural performance analysis

Posted Date: March 3rd, 2026

DOI: https://doi.org/10.21203/rs.3.rs-8931617/v1

License: This work is licensed under a Creative Commons Attribution 4.0 International License. Read Full License

Additional Declarations: No competing interests reported.

Abstract

Prestressed carbon fiber–reinforced polymer (CFRP) plate strengthening has been widely applied in the rehabilitation of flexural bridge members due to its advantages of low self-weight, convenient construction, and excellent durability. However, existing studies have mainly focused on the static behavior of prestressed CFRP-strengthened beams, while the flexural fatigue performance of prestressed CFRP plate–strengthened bridge girders remains insufficiently understood. To address this gap, this study investigates bridge T-beam members through a series of flexural fatigue tests, including unstrengthened beams, beams strengthened with non-prestressed CFRP plates, and beams strengthened with prestressed CFRP plates. The evolution of mid-span deflection, stiffness degradation, strain responses of tensile reinforcement and CFRP plates, as well as the interfacial bond behavior under different strengthening schemes were systematically analyzed. In addition, the effects of fatigue damage accumulation on the residual static performance and ultimate load-carrying capacity of prestressed CFRP-strengthened beams were further examined. The experimental results indicate that, compared with unstrengthened beams and non-prestressed CFRP-strengthened beams, prestressed CFRP plate–strengthened beams exhibited smaller mid-span deflections, more stable stiffness degradation characteristics, and lower strain amplitudes in tensile reinforcement during fatigue loading, demonstrating a significant improvement in flexural fatigue performance. In contrast, beams strengthened with non-prestressed CFRP plates were prone to CFRP–concrete interfacial debonding under cyclic loading, which led to stress redistribution between the steel reinforcement and CFRP plates, resulting in a rapid increase in reinforcement strain amplitude and premature fatigue failure. Post-fatigue monotonic loading tests further revealed that moderate fatigue damage had a limited influence on the static load capacity of prestressed CFRP-strengthened beams, whereas more pronounced degradation in stiffness and load-bearing performance occurred under higher fatigue load levels. Overall, the results demonstrate that prestressed CFRP plates can effectively reduce the stress level of tensile reinforcement while maintaining favorable interfacial bonding performance, thereby significantly enhancing the flexural fatigue resistance of bridge girder members. This study provides experimental evidence to support fatigue strengthening strategies for existing bridges.

1. Introduction

With the continuous increase in traffic load levels and the growing service life of bridges, girder bridges are prone to fatigue damage accumulation under repeated vehicular loading. This is typically manifested by stiffness degradation, increased deflection, and crack propagation, which severely compromise the service performance and durability of bridge structures. For existing small- and medium-span girder bridges, effectively enhancing their flexural fatigue resistance under the premise of maintaining traffic operation or minimizing interruptions has become an urgent issue in the field of bridge maintenance and strengthening [1–2].

Fiber-reinforced polymer (FRP) composites, characterized by high strength, low self-weight, and excellent corrosion resistance, have been widely employed in the flexural strengthening of concrete girder bridges. Among various techniques, externally bonded carbon fiber–reinforced polymer (CFRP) plate strengthening has gained extensive application in engineering practice due to its convenient installation and well-defined load-transfer mechanism [3–4]. Numerous studies have investigated the mechanical performance of reinforced concrete beams strengthened with externally bonded CFRP plates. The research conducted by Li et al. [5], Wang et al. [6], and Zhang et al. [7] demonstrated that non-prestressed CFRP plates can enhance the load-carrying capacity and improve the deformation behavior of beams to a certain extent; however, their strengthening effectiveness remains limited under service conditions. This limitation is mainly attributed to the relatively low elastic modulus of CFRP materials, which prevents their high-strength advantage from being fully mobilized during the deformation-restricted service stage. To overcome the restricted efficiency of non-prestressed CFRP strengthening, prestressed CFRP plate systems have gradually attracted increasing attention. Studies by El-Sayed [8], Zhou [9], and Wang [10] indicated that applying prestress to CFRP plates prior to bonding can significantly reduce the tensile stress level in reinforcing steel under service conditions and improve the strength utilization efficiency of CFRP materials. Experimental results have confirmed that prestressed CFRP plates outperform non-prestressed CFRP plates in terms of enhancing cracking resistance, reducing deflection, and increasing static load capacity. Regarding fatigue performance, existing studies generally agree that fatigue failure of reinforced concrete beams is primarily governed by the stress level of tensile reinforcement. After conducting fatigue tests on multiple reinforced concrete T-beams, Alam et al. [11] reported that strengthening with non-prestressed CFRP plates can extend the fatigue life of beams; nevertheless, the fatigue behavior is still mainly controlled by the fatigue performance of steel reinforcement, and the strengthening effectiveness is largely constrained by the bond quality at the CFRP–concrete interface. Corte et al. [12] observed in high-amplitude fatigue loading tests that some CFRP-strengthened beams experienced interfacial degradation and debonding failure before reaching the designed number of fatigue cycles. Furthermore, studies by Abdel [13] and Kueres [14] showed that stiffness degradation of CFRP-strengthened beams becomes more pronounced under the combined effects of fatigue loading and long-term adverse environmental conditions.

The aforementioned studies have, to some extent, revealed the fatigue behavior of beams strengthened with non-prestressed CFRP plates; however, research on the fatigue performance of prestressed CFRP plate–strengthened members remains relatively limited. Yuan et al. [15] conducted cyclic loading tests on RC slabs strengthened with prestressed CFRP plates and reported that fatigue failure is generally initiated by fracture of the tensile reinforcement, followed by interfacial debonding of the CFRP plate. Ghafoori [16] demonstrated that after two million fatigue cycles, the post-fatigue load-carrying capacity of prestressed CFRP-strengthened beams exhibited only a slight reduction, confirming the effectiveness of prestressing measures. Experimental results from Almassri [17] and Zhang [18] further indicated that, compared with non-prestressed CFRP systems, prestressed CFRP can more effectively reduce steel strain, concrete creep strain, and beam deflection, thereby significantly extending the fatigue life. Ye et al. [19] also found in fatigue strengthening studies of steel beams that the application of prestressed CFRP plates could increase the fatigue life by several times. It should be noted, however, that prestressed CFRP plate strengthening systems face additional challenges under fatigue loading, particularly with respect to end anchorage and the complex interfacial stress state. Al-Fakih [20] and Zhu [21] pointed out that increasing the prestress level leads to

a substantial rise in interfacial stresses near the CFRP plate ends, making interfacial degradation more likely under cyclic loading. Moreover, since epoxy adhesives alone are often unable to sustain the large force transfer associated with prestressing, permanent anchorage devices are typically required in practice. The presence of such anchorage systems further complicates the stress distribution among concrete, steel reinforcement, and CFRP plates. These factors collectively indicate that the fatigue behavior of prestressed CFRP plate–strengthened beams differs fundamentally from that of non-prestressed systems, highlighting the necessity for systematic and targeted investigations.

Based on the above research background, this study investigates bridge T-beam members through a comprehensive flexural fatigue experimental program, including unstrengthened beams, beams strengthened with non-prestressed CFRP plates, and beams strengthened with prestressed CFRP plates. By systematically monitoring the mid-span deflection, stiffness degradation, strain responses of tensile reinforcement and CFRP plates, as well as the CFRP–concrete interfacial behavior, the fatigue response characteristics and failure modes of beams under different strengthening schemes are analyzed. Furthermore, post-fatigue monotonic loading tests are conducted to evaluate the effects of fatigue damage accumulation on the static performance and residual load-carrying capacity of prestressed CFRP-strengthened beams. The findings are expected to provide experimental evidence for the flexural fatigue performance assessment and practical application of prestressed CFRP plate strengthening in existing girder bridge members.

2. Flexural Fatigue Tests of Beams

2.1 Specimen Design and Test Conditions

The beam specimens had an overall length of 5.0 m with a calculated span of 4.8 m. The beam depth was 600 mm, while the flange width and thickness were 600 mm and 100 mm, respectively, and the web thickness was 200 mm. The geometric dimensions and reinforcement arrangement of the specimens are illustrated in Fig. 1.

To investigate the flexural fatigue performance of reinforced concrete T-beam members strengthened with prestressed CFRP plates, a total of three RC T-beam specimens were fabricated in this study. The corresponding test conditions are summarized in Table 1.

Table 1
Test conditions

Specimen number	Strengthening condition	Prestressing stress/MPa
1	Not strengthened	-
2	Strengthened	0
3	Strengthened	1000

2.2 Material Properties

The concrete used for the beam specimens was designed with a target strength grade of C40, and the corresponding mix proportions are provided in Table 2. All concrete specimens were cast simultaneously, and the measured 28-day cubic compressive strength was 41.2 MPa.

Table 2
Mix proportions of concrete

P.O 42.5 Cement/kg	Water/kg	Medium Sand/kg	Stone (5–20 mm continuously graded aggregate)/kg
440	170	680	1100

The longitudinal reinforcement and stirrups used in the beam specimens were of strength grades HRB400 and HPB235, respectively, and their measured mechanical properties are summarized in Table 3.

Table 3
Material properties

Material	Parameter	Value
Concrete	cubic compressive strength	41.2 MPa
	elastic modulus	33.1 GPa
	Poisson's ratio	0.19
	density	2409 kg/m^3
Rebar	yield strength (HRB400)	421 MPa
	yield strength (HPB235)	265 MPa
	tensile strength (HRB400)	573 MPa
	tensile strength (HPB235)	384 MPa
CFRP plate	width	100 mm
	thickness (single layer)	2 mm
	tensile strength	2900 MPa
	elastic modulus	170 GPa
Epoxy resin adhesive	bonding strength	13.5 MPa

2.3 Installation of Prestressed CFRP Plates

The CFRP plates were bonded to the soffit of the beam specimens, centrally aligned along the longitudinal axis, with a bonded length of 3.6 m. The prestressed CFRP plates were connected to the end anchorage devices through corrugated clamping plates, as shown in Fig. 2. The end anchorage systems were fixed to the beam ends using chemical anchor bolts. The anchorage devices were selected from a commonly used commercial product available in the domestic market, as illustrated in Fig. 2. The CFRP plates were first tensioned to the target prestressing level using a hydraulic jack, and then bonded to the concrete surface. During the bonding process, the target prestress level was maintained.

For the non-prestressed CFRP plate–strengthened beam (Specimen 2), anchorage devices were installed at both ends of the CFRP plate to provide mechanical fixation and to prevent interfacial debonding between the CFRP plate and the concrete surface [7–8].

To ensure reliable prestress transfer and stable bond performance, the installation of the prestressed CFRP plates followed a controlled and standardized procedure. Prior to bonding, the concrete soffit within the designated bond length was mechanically roughened to remove laitance and contaminants, and the surface was cleaned to ensure adequate adhesion. Any local surface defects were repaired to obtain a sound bonding substrate. Prestressing was applied using a hydraulic jack connected to the active-end anchorage system, while the opposite end was fixed by a passive anchorage. A dual-control method was adopted, in which both the applied jack force and the measured CFRP strain were monitored to achieve the target prestress level (1000 MPa). The prestress was applied incrementally to minimize seating losses and anchorage slip. After reaching the target level, the prestress was maintained for a stabilization period to ensure stress uniformity before bonding operations were finalized. The epoxy adhesive was prepared according to the manufacturer's specified mixing ratio and applied uniformly to the prepared concrete surface. The CFRP plate was bonded while maintaining the target prestress level to ensure effective stress transfer. During curing, the bonded region was protected from external disturbances, and sufficient curing time was allowed under ambient laboratory conditions before removing the prestressing equipment. The end anchorage system consisted of steel clamping plates and chemical anchor bolts installed at the beam ends. High-strength bolts were tightened in a symmetric sequence to ensure uniform clamping pressure. This configuration enhanced force transfer efficiency and mitigated stress concentration near the laminate ends under fatigue loading.

2.4 Test Loading and Measurements

As shown in Fig. 1, the flexural fatigue tests were conducted under a four-point bending configuration. The loading span was 4800 mm, and the shear span length was 2100 mm. The loading setup and reaction frame are illustrated in Fig. 3.

A constant-amplitude sinusoidal cyclic load was applied with the mean load as the reference level. The minimum and maximum loads were set to 10 kN and 50 kN, respectively, and the loading frequency was 5 Hz. The applied load was monitored and controlled using a load cell installed between the hydraulic jack and the loading beam.

According to relevant studies, a total of seven dial gauges were installed to measure the beam deflections, as shown in Fig. 4. Electrical resistance strain gauges with a gauge length of 5 mm were attached at the mid-span of the longitudinal reinforcement to monitor the steel strain. In addition, twenty-five electrical resistance strain gauges, each with a gauge length of 5 mm, were bonded to the surface of the CFRP plate to measure the strain distribution along the tensile direction, as illustrated in Fig. 4.

In addition, four and six electrical resistance strain gauges with a gauge length of 100 mm were bonded to the compression zone and the side surfaces of the beam specimens, respectively, to measure the concrete compressive strain and to analyze the strain distribution along the beam depth.

3. Experimental Results

The experimental results are summarized in Table 4.

Table 4
Test results

Specimen number	$\varepsilon_{max,rebar}/10^{-6}$	$\varepsilon_{min,rebar}/10^{-6}$	$\Delta\varepsilon_{rebar}/10^{-6}$	$\varepsilon_{max,CFRP}/10^{-6}$	$\varepsilon_{min,CFRP}/10^{-6}$	$\Delta\varepsilon_{CFRP}/10^{-6}$	δ_1/mm	Max cycle	Failure mode
1	1029	50	979	-	-	-	7.6	22.7×10^4	reinforcement fracture
2	964	254	710	771	138	633	5.7	70.2×10^4	reinforcement fracture after CFRP debonding
3	531	75	456	708	134	574	4.5	10^6	monotonically loaded to failure after 200×10^4 cycles

Note: In Table 4, $\varepsilon_{max,rebar}$ and $\varepsilon_{min,rebar}$ denote the maximum and minimum strains of the tensile reinforcement, respectively, and $\Delta\varepsilon_{rebar}$ represents the strain range of the reinforcement. Similarly, $\varepsilon_{max,CFRP}$ and $\varepsilon_{min,CFRP}$ denote the maximum and minimum strains of the CFRP plate, respectively, and $\Delta\varepsilon_{CFRP}$ represents the strain range of the CFRP plate. In addition, δ_1 refers to the beam deflection corresponding to the maximum load in the first loading cycle.

3.1 Fatigue Behavior

Figure 5 presents the variation of mid-span deflection with the number of loading cycles for Specimen 1 (the unstrengthened control beam) during the fatigue test.

As shown in Fig. 5, the mid-span deflection of Specimen 1 increased significantly within the first 10^4 loading cycles, indicating the accumulation of internal damage in the beam under cyclic loading. During the subsequent range of $(1–2)\times10^4$ cycles, a slight reduction in deflection was observed. Thereafter, the deflection exhibited a continuous increasing trend over the cycle range of $(2–10)\times10^4$. When the number of cycles reached 22.7×10^4, fracture of the longitudinal tensile reinforcement occurred, leading to the failure of Specimen 1.

The variation of mid-span deflection with the number of cycles for Specimen 2 (the beam strengthened with a non-prestressed CFRP plate) is shown in Fig. 7. The mid-span deflection continuously increased as the fatigue cycles progressed. During the first loading cycle, the maximum strain of the longitudinal tensile reinforcement in Specimen 2 under the peak load reached 964 με, which was 79.8% of that recorded in Specimen 1. After 50×10^4 cycles, debonding between the CFRP plate and the concrete surface was observed near the loading point, as illustrated in Fig. 8. With further increase in the number of cycles, the debonded region propagated toward both supports and eventually developed into overall debonding of the CFRP plate from the soffit concrete surface. At this stage, the CFRP plate was only mechanically retained by the steel anchorage devices. When the number of cycles reached 70.2×10^4, fatigue fracture of the longitudinal tensile reinforcement occurred at the beam bottom, leading to the failure of Specimen 2.

Specimen 3 (the beam strengthened with a prestressed CFRP plate) was initially prestressed to a level of 1000 MPa. The growth curve of mid-span deflection with increasing fatigue cycles is presented in Fig. 7. Within the first 10^4 loading cycles, the mid-span deflection of Specimen 3 increased rapidly, indicating significant internal damage accumulation in the beam under cyclic loading [5, 17, 22]. Thereafter, the mid-span deflection exhibited a gradual growth up to 160×10^4 cycles. During the subsequent cycle range of $(160–200)\times10^4$, the deflection growth rate increased noticeably, showing a pronounced rise.

3.2 Deformation Analysis

By comparing the curves of Specimens 2 and 3 in Fig. 7, it can be observed that the beam strengthened with a prestressed CFRP plate (Specimen 3) exhibited a significant advantage in flexural fatigue resistance. For Specimen 2, the mid-span deflection under the maximum load of the first loading cycle ($\delta1$) was 5.7 mm, and the deflection continued to increase with the number of cycles until failure occurred. In contrast, under the same fatigue loading conditions, Specimen 3 showed a markedly lower deflection level during the first 150×10^4 cycles. Moreover, it should be emphasized that after the rapid increase in mid-span deflection during the initial 10^3 cycles, the deflection of Specimen 3 remained relatively stable, whereas the mid-span deflection of Specimen 2 exhibited a continuous growth trend throughout the fatigue loading process.

Figure 9 illustrates the variation of stiffness with the number of fatigue cycles for Specimens 2 and 3. It can be seen that the stiffness of Specimen 2 decreased significantly after the first 10^5 loading cycles, and it continued to decline throughout the subsequent fatigue loading process until failure occurred. This indicates that cyclic fatigue loading induces pronounced damage accumulation in beams strengthened with non-prestressed CFRP plates (Specimen 2) [9, 12].

Similarly, the stiffness of Specimen 3 initially increased and then decreased rapidly within the first 10^5 loading cycles, which is consistent with the observed variation in mid-span deflection. After the rapid reduction stage, the stiffness of Specimen 3 exhibited a gradual decline up to 160×10^4 cycles, while remaining at a relatively stable level. This suggests that cyclic fatigue loading did not induce pronounced damage accumulation within the beam during this stage. However, during the subsequent cycle range of $(160–200)\times10^4$, a sudden stiffness drop was observed. This phenomenon agrees well with the corresponding deflection development, reflecting the structural performance degradation of the prestressed CFRP plate–strengthened beam (Specimen 3) under fatigue loading [1–2, 4, 23].

3.3 Strain Analysis

Figure 10 presents the variation of the strain range of the bottom tensile reinforcement ($\Delta\varepsilon_{rebar}$) and the strain range of the CFRP plate ($\Delta\varepsilon_{CFRP}$) with increasing fatigue cycles for Specimens 2 and 3. As shown in Fig. 10(a), the strain range of the tensile reinforcement in Specimen 2 increased significantly with the number of cycles, which can be attributed to CFRP–concrete interfacial debonding and the associated stress redistribution. In contrast, as indicated in Fig. 10(b), throughout the entire fatigue loading process, the evolution trend of the CFRP plate strain range in Specimen 3 remained consistent with that of the tensile reinforcement. This suggests that the CFRP plate maintained a favorable bonding condition with the soffit concrete surface during fatigue loading [6, 16].

Figure 10(c) compares the evolution of the strain range of the bottom tensile reinforcement with the number of fatigue cycles for Specimens 2 and 3. It can be observed that throughout the entire fatigue loading process, the tensile reinforcement strain range of Specimen 3 remained consistently lower than that of Specimen 2. At 50×10^4 cycles, the strain range of Specimen 2 was approximately 1.6 times that of Specimen 3. Specimen 2 failed after 70.2×10^4 cycles due to fatigue fracture of the tensile reinforcement, whereas Specimen 3 did not exhibit failure even after 200×10^4 cycles. These results indicate that prestressed CFRP plate strengthening can effectively reduce the stress level of tensile reinforcement and significantly enhance the flexural fatigue resistance of reinforced concrete T-beams [3, 7–8]. In contrast, non-prestressed CFRP plates tend to lose their bond with the concrete surface under cyclic fatigue loading, and therefore cannot provide effective strengthening for T-beam members [5, 24].

To further elucidate the underlying mechanism governing the different strain evolution behaviors between prestressed and non-prestressed CFRP strengthening systems, the interfacial stress transfer mechanism and bond–slip interaction should be considered. According to bond mechanics principles, the interfacial shear stress between the CFRP plate and concrete substrate can be approximately expressed as:

$$\tau\ (x) = \frac{E_f t_f}{b_f} \bullet \frac{d\epsilon\ _f\,(x)}{dx}$$

where E_f and t_f denote the elastic modulus and thickness of the CFRP plate, respectively, bf is the plate width, and $d\varepsilon_f/dx$ represents the strain gradient along the bonded length. This relationship indicates that local interfacial shear stress is directly governed by the spatial variation of CFRP strain.

For the non-prestressed CFRP-strengthened beam, the initial interfacial stress is negligible prior to loading. Under cyclic bending, tensile force transfer from concrete to CFRP leads to progressive strain localization near the loading region, resulting in high shear stress concentration at the interface. As fatigue cycles accumulate, microcracking and interfacial slip initiate and propagate, eventually causing partial debonding. Once debonding occurs, the tensile force previously carried by the CFRP plate is redistributed to the steel reinforcement, leading to a sharp increase in reinforcement strain range and accelerating fatigue fracture.

In contrast, the prestressed CFRP system introduces an initial compressive stress state in the concrete and an initial tensile stress in the CFRP plate before external loading is applied. This prestress reduces the effective tensile stress amplitude experienced by the reinforcement under cyclic loading and modifies the strain gradient distribution along the bonded length. As a result, interfacial shear stress peaks are mitigated and more uniformly distributed. From a bond–slip perspective, prestressing delays the development of relative slip between the CFRP plate and concrete substrate, thereby restraining damage evolution within the interfacial transition zone.

The schematic comparison of interfacial stress distribution and bond–slip behavior between the two strengthening systems is illustrated in Fig. 11. It can be inferred that prestressing effectively stabilizes the load transfer mechanism, alleviates stress redistribution triggered by local debonding, and maintains coordinated deformation between CFRP and reinforcement. This mechanism explains why the prestressed CFRP-strengthened beam exhibited a consistently lower reinforcement strain range and a significantly extended fatigue life.

From the perspective of interfacial mechanics, the different fatigue responses between non-prestressed and prestressed CFRP systems can be further explained by bond deterioration and stress redistribution mechanisms. In the non-prestressed configuration, the interface initially carries no prestress, and cyclic loading promotes progressive slip accumulation near high-moment regions. Once partial debonding initiates, tensile force previously transferred to the CFRP plate is redistributed to the steel reinforcement, resulting in a rapid increase in reinforcement strain range and accelerated fatigue crack propagation. In contrast, prestressing introduces an initial tensile stress in the CFRP plate and a compressive state in the concrete

substrate, which reduces the effective tensile stress amplitude in the reinforcement and mitigates interfacial shear stress concentration. Consequently, slip development and debonding are delayed, stabilizing the load transfer mechanism and contributing to the improved fatigue resistance of the prestressed strengthening system.

3.4 Failure Loading

After undergoing 200×10^4 fatigue loading cycles, no debonding cracks were observed between the CFRP plate and the soffit concrete surface, nor was any fracture of the bottom longitudinal tensile reinforcement detected. Subsequently, to further investigate the influence of fatigue damage accumulation on the static performance and residual load-carrying capacity of the prestressed CFRP plate–strengthened T-beam, Specimen 3 was subjected to monotonic loading until failure. The corresponding response curves are presented in Fig. 12.

For Specimen 3, yielding of the bottom longitudinal tensile reinforcement occurred when the applied load reached 175 kN. As the load increased to 205 kN, debonding between the CFRP plate and the soffit concrete surface initiated at the mid-span region. The debonding crack then rapidly propagated toward the steel anchorage devices at both beam ends and extended throughout the entire bonded length. At this stage, the CFRP plate was connected to the beam only through the end steel anchorages, which carried the total tensile force in the CFRP plate. Similar to Specimen 2, after CFRP plate debonding occurred, both the mid-span deflection and the CFRP plate strain of Specimen 3 increased significantly. When the load further increased to 215 kN, failure took place due to tensile rupture of the anchorage bolts at one end, causing the steel anchorage device to be pulled out from the beam. The corresponding failure pattern is shown in Fig. 13.

As mentioned above, Specimen 3 exhibited damage accumulation during the cycle range of $(16–20)\times10^4$. Figure 12 indicates that the existing accumulated damage had a noticeable influence on the static behavior of Specimen 3 [11, 14].

4. Conclusions

Based on the flexural fatigue experimental investigation of unstrengthened reinforced concrete T-beams, T-beams strengthened with non-prestressed CFRP plates, and T-beams strengthened with prestressed CFRP plates under constant-amplitude cyclic loading, the effects of different strengthening schemes on the evolution of mid-span deflection, stiffness degradation characteristics, strain responses of tensile reinforcement and CFRP plates, as well as interfacial bonding performance were systematically analyzed. In addition, monotonic loading tests were conducted on the prestressed CFRP-strengthened beams after fatigue loading to further evaluate the influence of fatigue damage accumulation on the static performance and residual load-carrying capacity of the members. On this basis, combined with the observed fatigue failure modes and the evolution of key mechanical parameters, the enhancement mechanisms of flexural fatigue performance provided by prestressed CFRP plate strengthening were comprehensively discussed. The main conclusions can be drawn as follows:

(1) Compared with the unstrengthened beam and the beam strengthened with a non-prestressed CFRP plate, the prestressed CFRP plate–strengthened beam exhibited smaller mid-span deflections, more stable stiffness degradation behavior, and lower tensile reinforcement strain levels during fatigue loading. Under comparable or even higher fatigue load levels, the fatigue life of the prestressed CFRP-strengthened beam was significantly extended, whereas the non-prestressed CFRP-strengthened beam failed due to fatigue fracture of the tensile reinforcement after approximately 70.2×10^4 cycles.

(2) The experimental results showed that throughout the fatigue loading process, the strain range of the CFRP plate in the prestressed CFRP-strengthened beam evolved consistently with that of the tensile reinforcement, and no significant interfacial debonding was observed. In contrast, the non-prestressed CFRP-strengthened beam experienced progressive CFRP–concrete interfacial debonding under cyclic loading, which induced stress redistribution from the CFRP plate to the steel reinforcement. This redistribution led to a pronounced increase in reinforcement strain range and accelerated fatigue crack propagation in the steel bars. The introduction of prestress effectively reduced the tensile stress amplitude in the reinforcement and delayed the development of interfacial slip and debonding, thereby stabilizing the load transfer mechanism and enhancing the flexural fatigue resistance of the strengthened beam.

(3) Post-fatigue monotonic loading tests indicated that the prestressed CFRP plate–strengthened beam exhibited a load–carrying behavior prior to steel yielding that was generally consistent with that of the corresponding beam subjected to monotonic loading only, suggesting that moderate fatigue damage had a limited influence on its overall load capacity. However, under higher fatigue load levels and larger load amplitudes, the yielding load and the interfacial debonding load were significantly reduced, accompanied by accelerated stiffness degradation. Overall, prestressed CFRP plate strengthening demonstrates good engineering applicability for enhancing the flexural fatigue performance of existing girder bridge members.

Declarations

Funding Declaration

This research was supported by the Science and Technology Research Program of Chongqing Municipal Education Commission (Grant No.KJZD-K202503402, KJZD-K202505801), sponsored by Natural Science Foundation of Chongqing,China (Grant No.CSTB2025NSCQ-GPX0797).

Author Contributions

Qiang Lu: Supervision; Validation; Writing – Review & Editing.

Fengbing Zhao: Conceptualization; Methodology; Investigation; Data Curation; Writing – Original Draft.

Bolin Jiang: Resources; Visualization; Formal Analysis.

Shanshan Wu: Software; Experimental Setup; Data Processing.

All authors have read and approved the final version of this manuscript.

Data availability

Data will be made available on request.

Declaration of Competing Interest

The authors declare that they have no known competing financial interests or personal relationships that could have appeared to influence the work reported in this paper.

Ethical approval

Not applicable

Consent to publish

Not applicable

Clinical trial

Not applicable

References

1. Wang, H. T. et al. Flexural strengthening of damaged steel beams with prestressed CFRP plates using a novel prestressing system. *Eng. Struct.* **284**, 115953 (2023).
2. Li, A., Wang, H., Li, H., Kong, D. & Xu, S. Stress concentration analysis of the corroded steel plate strengthened with carbon fiber reinforced polymer (CFRP) plates. *Polymers* **14**, 3845 (2022).
3. Abdel Havez, A. & Al-Mayah, A. Flexural strengthening of concrete structures using externally bonded and unbonded prestressed CFRP laminates: A literature review. *J. Compos. Constr.* **27**, (2023).
4. Zhou, C., Wang, L., Wang, Y. & Fang, Z. Experimental study on the flexural strengthening of one-way RC slabs with end-buckled and/or externally bonded CFRP sheets. *Eng. Struct.* **282**, 115832 (2023).
5. Li, J., Zhu, M. & Deng, J. Flexural behaviour of notched steel beams strengthened with a prestressed CFRP plate subjected to fatigue damage and wetting/drying cycles. *Eng. Struct.* **250**, 113430 (2022).
6. Wang, H. T. et al. Structural performance of steel beams strengthened with prestressed CFRP plates: Steel beam-CFRP plate string systems. *Thin-Walled Struct.* **220**, 114251 (2026).
7. Zhang, W., Kang, S., Liu, X., Lin, B. & Huang, Y. Experimental study of a composite beam externally bonded with a carbon fiber-reinforced plastic plate. *J. Building Eng.* **71**, 106522 (2023).
8. El-Sayed, A. K., Al-Zaid, R. A., Al-Negheimish, A. I., Shuraim, A. B. & Alhozaimy, A. M. Long-term behavior of wide shallow RC beams strengthened with externally bonded CFRP plates. *Constr. Build. Mater.* **51**, 473–483 (2014).
9. Zhou, C. Y., Yu, Y. N. & Xie, E. L. Strengthening RC beams using externally bonded CFRP sheets with end self-locking. *Compos. Struct.* **241**, 112070 (2020).
10. Wang, Q. et al. Fatigue performance of CFRP reinforced pretensioned prestressed beams. *Constr. Build. Mater.* **324**, 126509 (2022).
11. Alam, M. A., Onik, S. A. A. & Mustapha, K. N. B. Crack-based bond strength model of externally bonded steel plate and CFRP laminate to predict debonding failure of shear-strengthened RC beams. *J. Building Eng.* **27**, 100943 (2020).
12. De Corte, W. & Van Bogaert, P. Evaluation of an experimental CFRP prestressed beam and slab road bridge. *Compos. Part. B.* **36**, 91–98 (2005).
13. Abdel Havez, A. & Al-Mayah, A. High prestressing of externally mounted CFRP plates for prestressed hollow-core slabs strengthening. *Structures* **75**, 108698 (2025).
14. Kueres, S. & Hegger, J. Reliability analysis of footbridges pre-tensioned with carbon fiber reinforced polymer tendons under flexural loading. *Eng. Struct.* **203**, 109546 (2020).
15. Yuan, X., Zhu, C., Zheng, W., Hu, J. & Tang, B. Flexure performance of externally bonded CFRP plate-strengthened reinforced concrete members. Mathematical Problems in Engineering 2604024 (2020). (2020).

16. Ghafoori, E. et al. Finite element analysis for fatigue damage reduction in metallic riveted bridges using prestressed CFRP plates. *Polymers* **6**, 1096–1118 (2014).
17. Almassri, B., Halahla, A. M. & Corroded RC beam repaired in flexure using NSM CFRP rod and an external steel plate. *Structures* **27**, 343–351 (2020).
18. Zhang, Z. J. et al. Entire mechanical analysis of prestressed CFRP strengthened RC beams under different prestress introduction methods. *Adv. Bridge Eng.* **5**, 13 (2024).
19. Ye, H. et al. Fatigue performance analysis of damaged steel beams strengthened with prestressed unbonded CFRP plates. *J. Bridge Eng.* **23**, 04018040 (2018).
20. Al-Fakih, A. et al. Cracking behavior of sea sand RC beam bonded externally with CFRP plate. *Structures* **33**, 1578–1589 (2021).
21. Zhu, K. Research on prestressed CFRP plate in the reinforcement of composite box girder bridge. Journal of Physics: Conference Series 2920, 012013 (2024).
22. Cheng, X. et al. Seismic response of a box bridge after reinforcement with prestressed CFRP textile. *Australian J. Civil Eng.* **18**, 29–45 (2019).
23. Hu, L., Li, W. & Feng, P. Long-term behavior of CFRP plates under sustained loads. *Adv. Struct. Eng.* **25**, 939–953 (2022).
24. Wang, H. T. & Wu, G. Bond-slip models for CFRP plates externally bonded to steel substrates. *Compos. Struct.* **184**, 1204–1214 (2018).

Figures

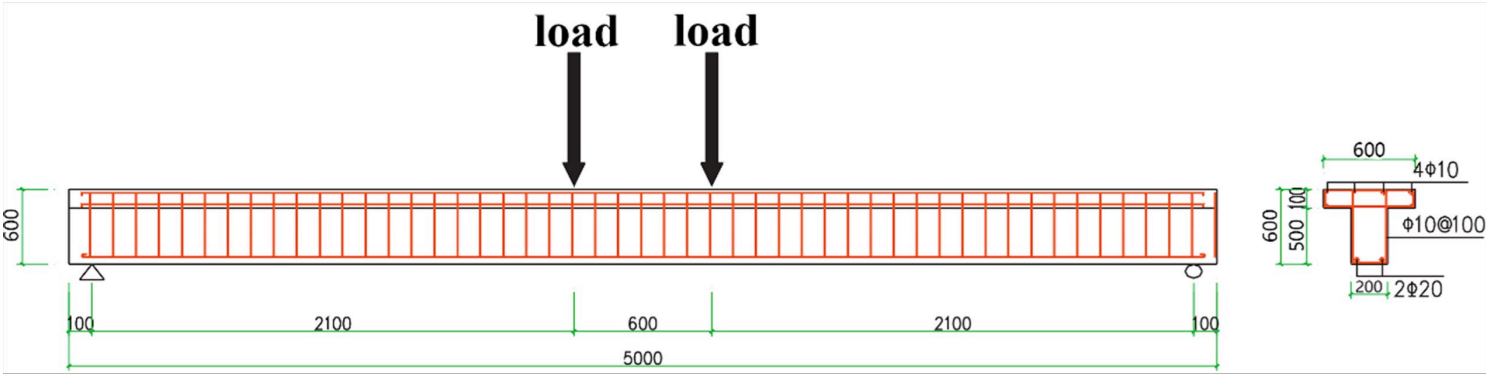


Figure 1

Diagram of beam specimens

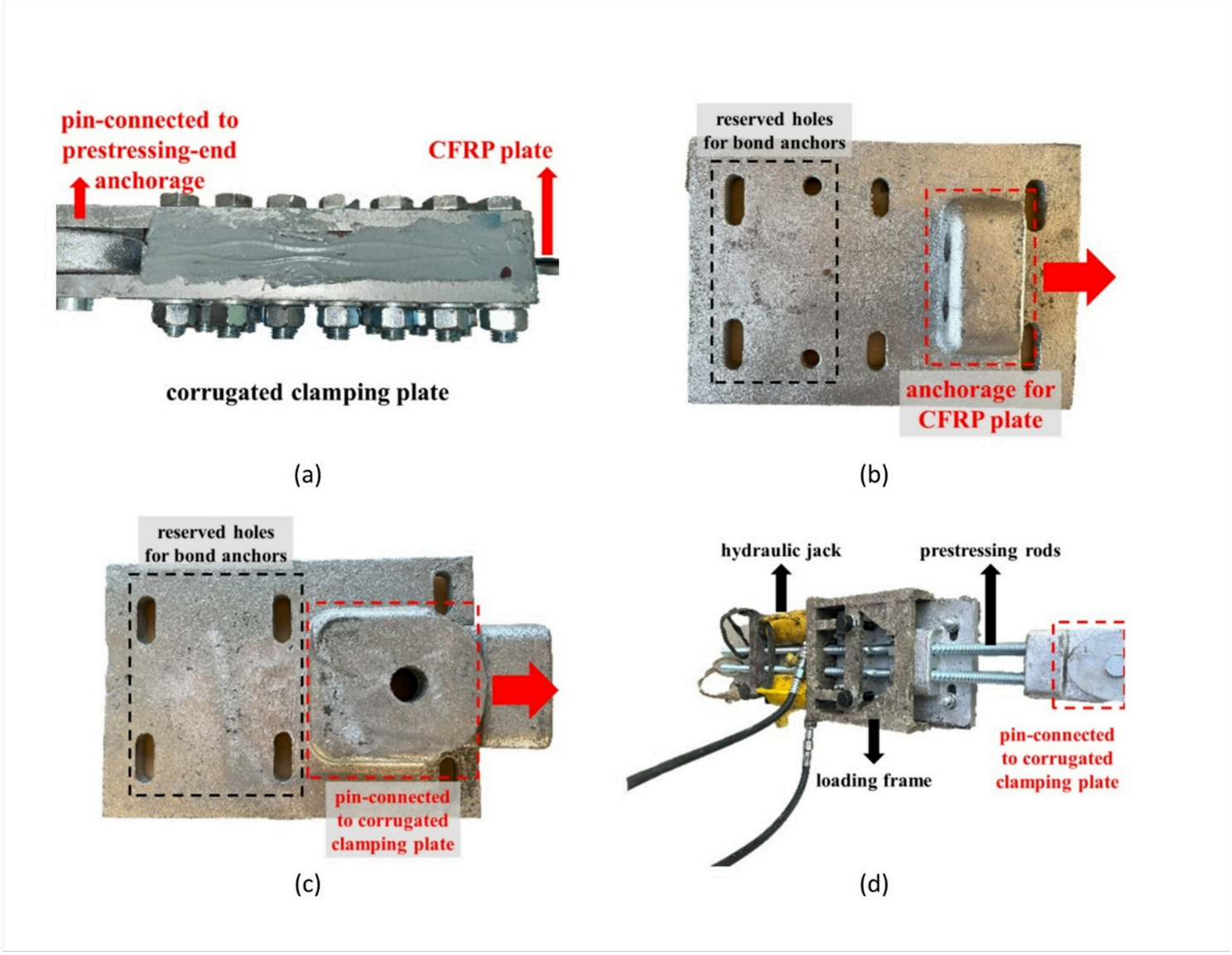


Figure 2

End anchorage: (a) corrugated clamping plate, (b) fix-end anchorage, (c) prestressing-end anchorage and (d) prestressed CFRP plate



Figure 3

Test loading device

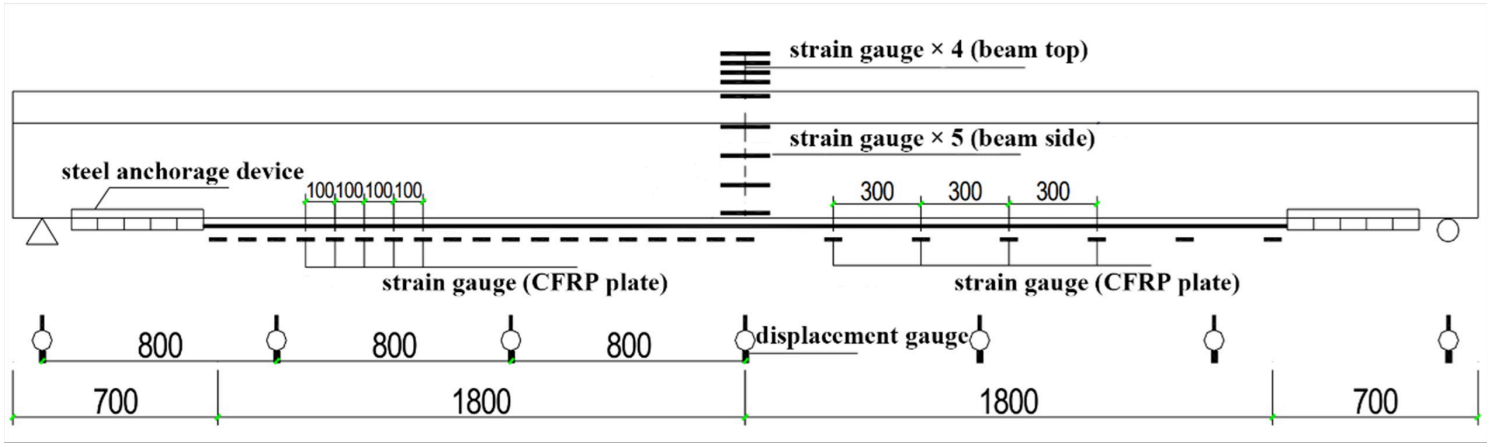


Figure 4

Measurement layout

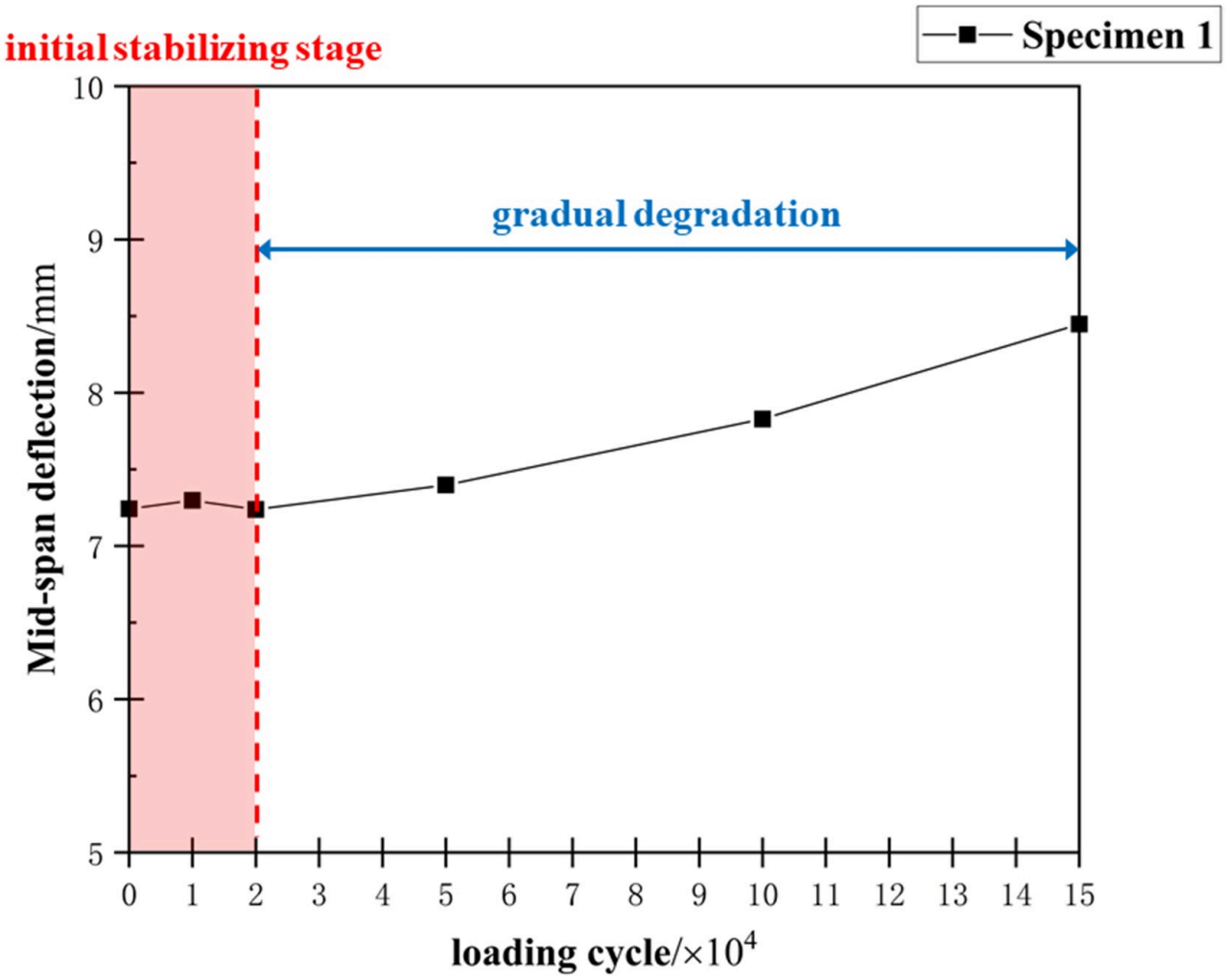


Figure 5

Mid-span deflection versus number of loading cycles for Specimen 1

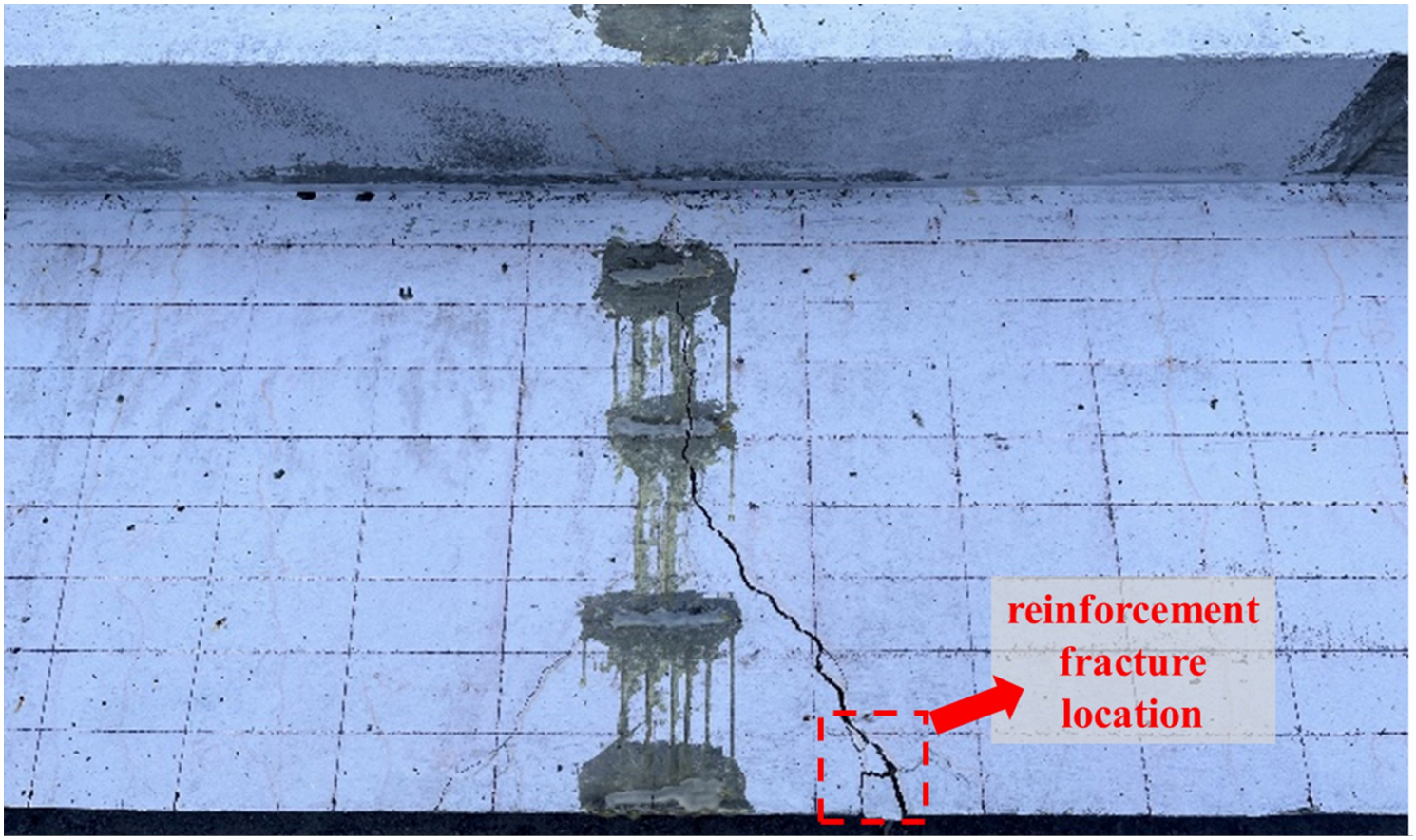


Figure 6

Failure for Specimen 1

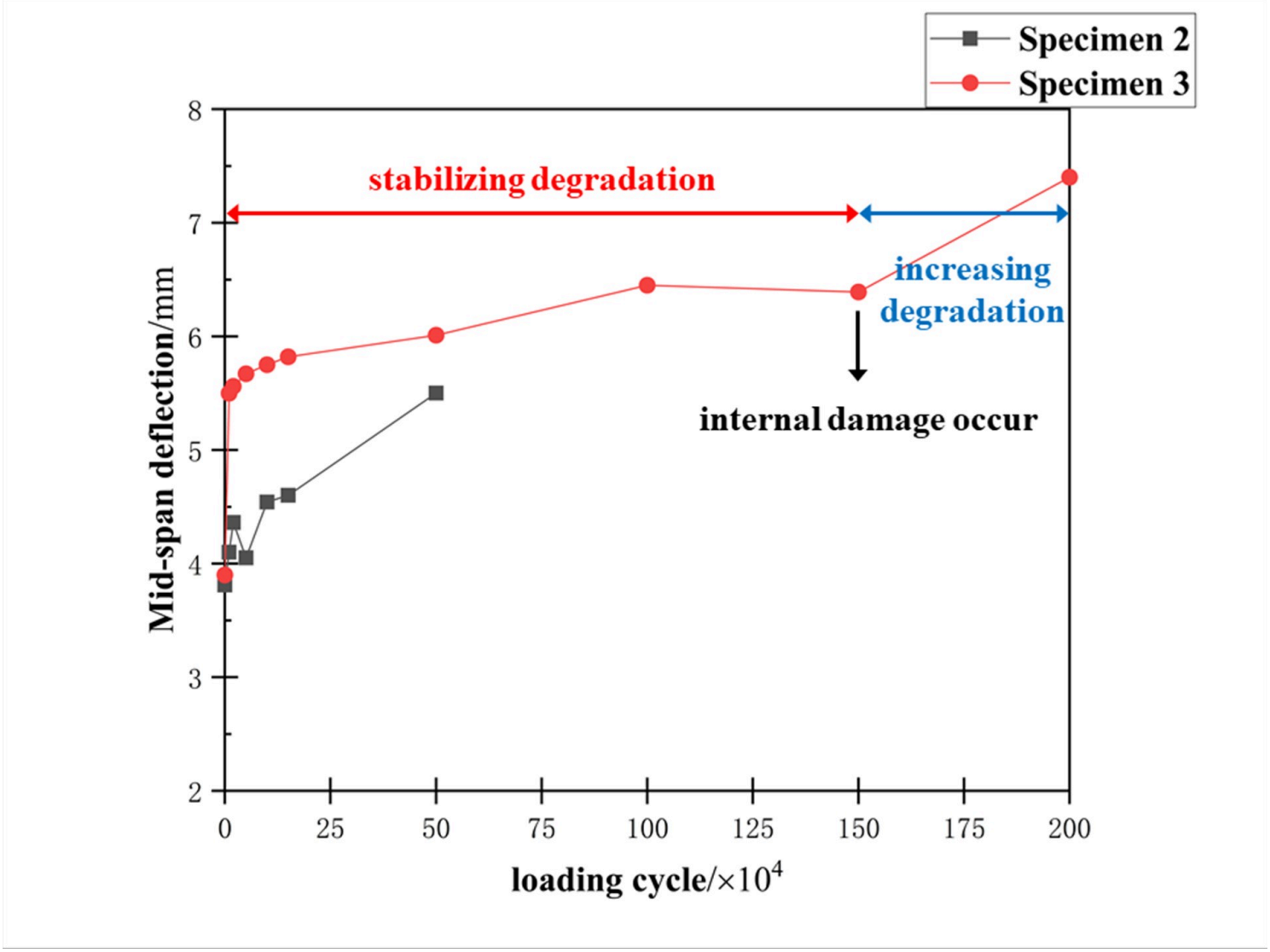


Figure 7

Mid-span deflection versus number of loading cycles for Specimen 2 and Specimen 3

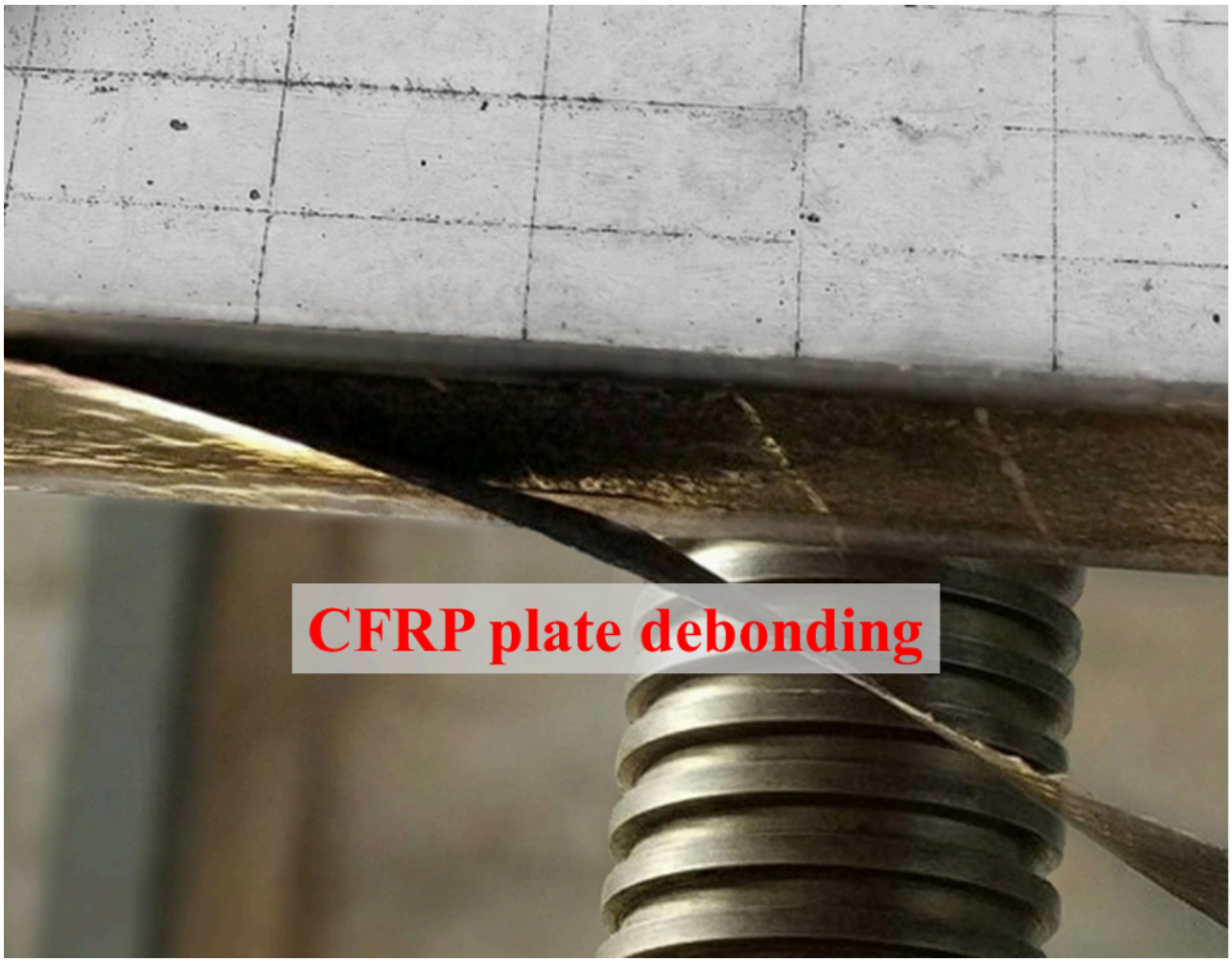


Figure 8

Peeling of CFRP plate

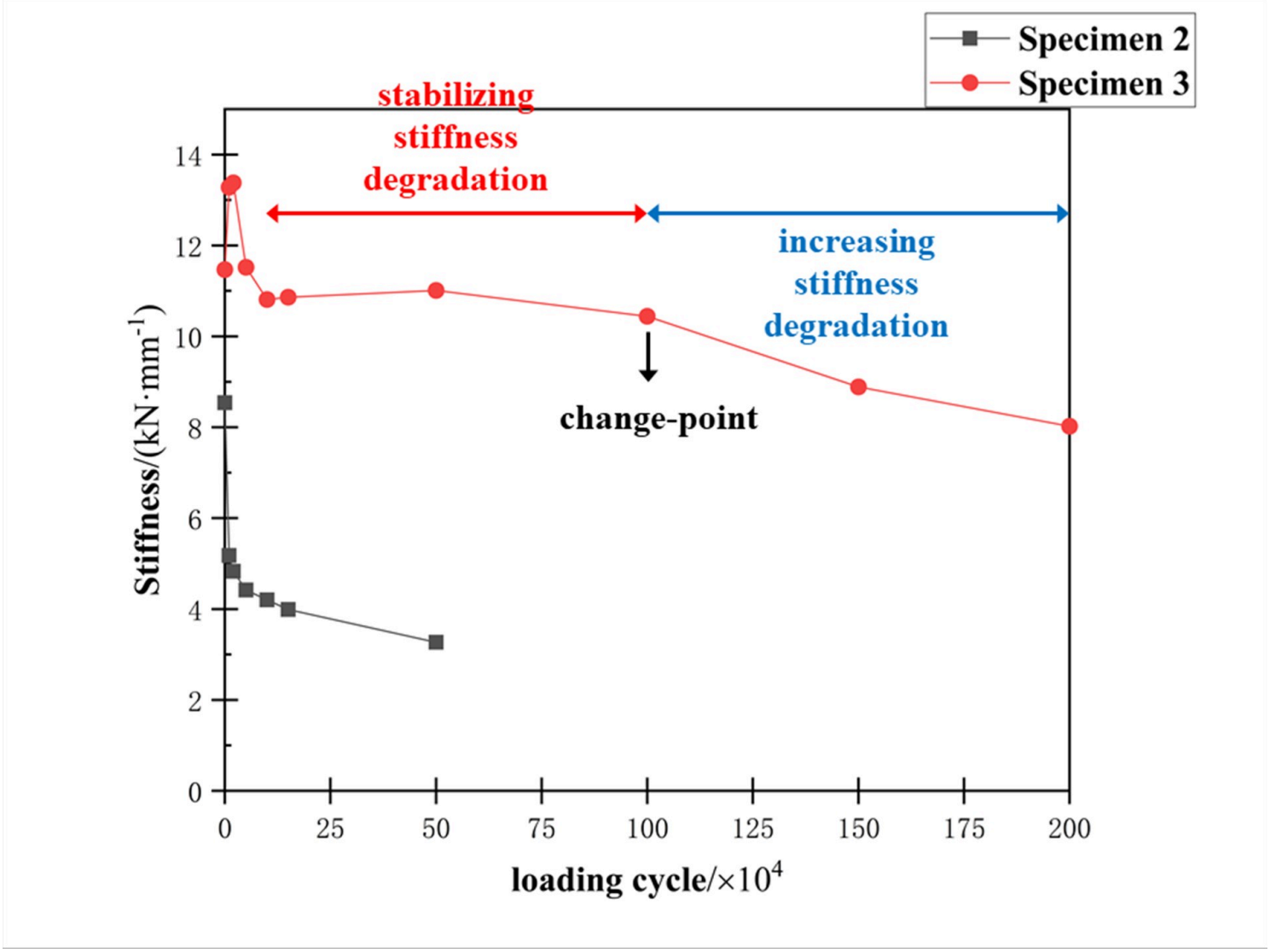


Figure 9

Stiffness versus number of loading cycles

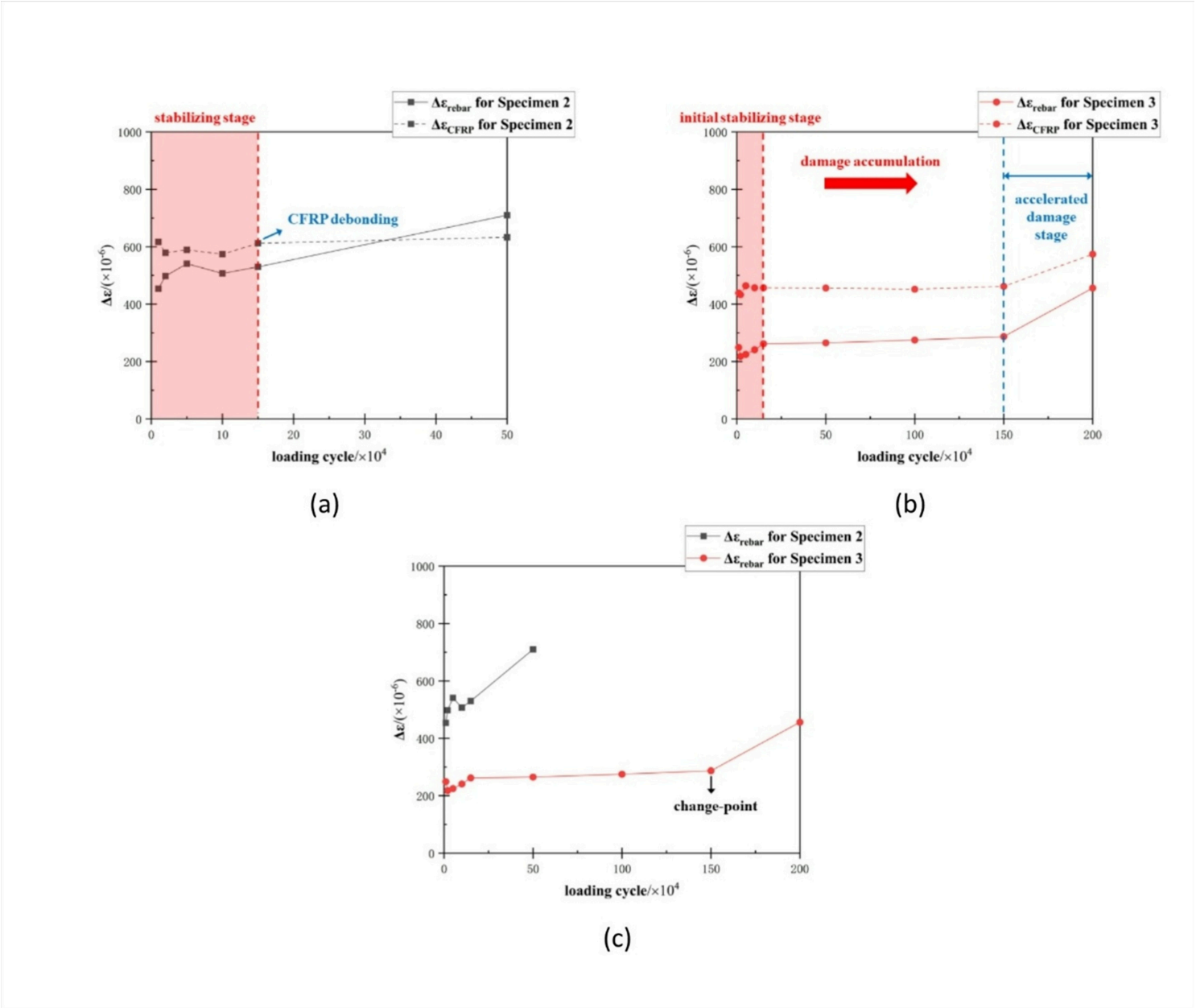


Figure 10

Strain of marterials versus number of loading cycles: (a) Specimen 2, (b) Specimen 3 and (c) comparison between Specimen 2 and 3

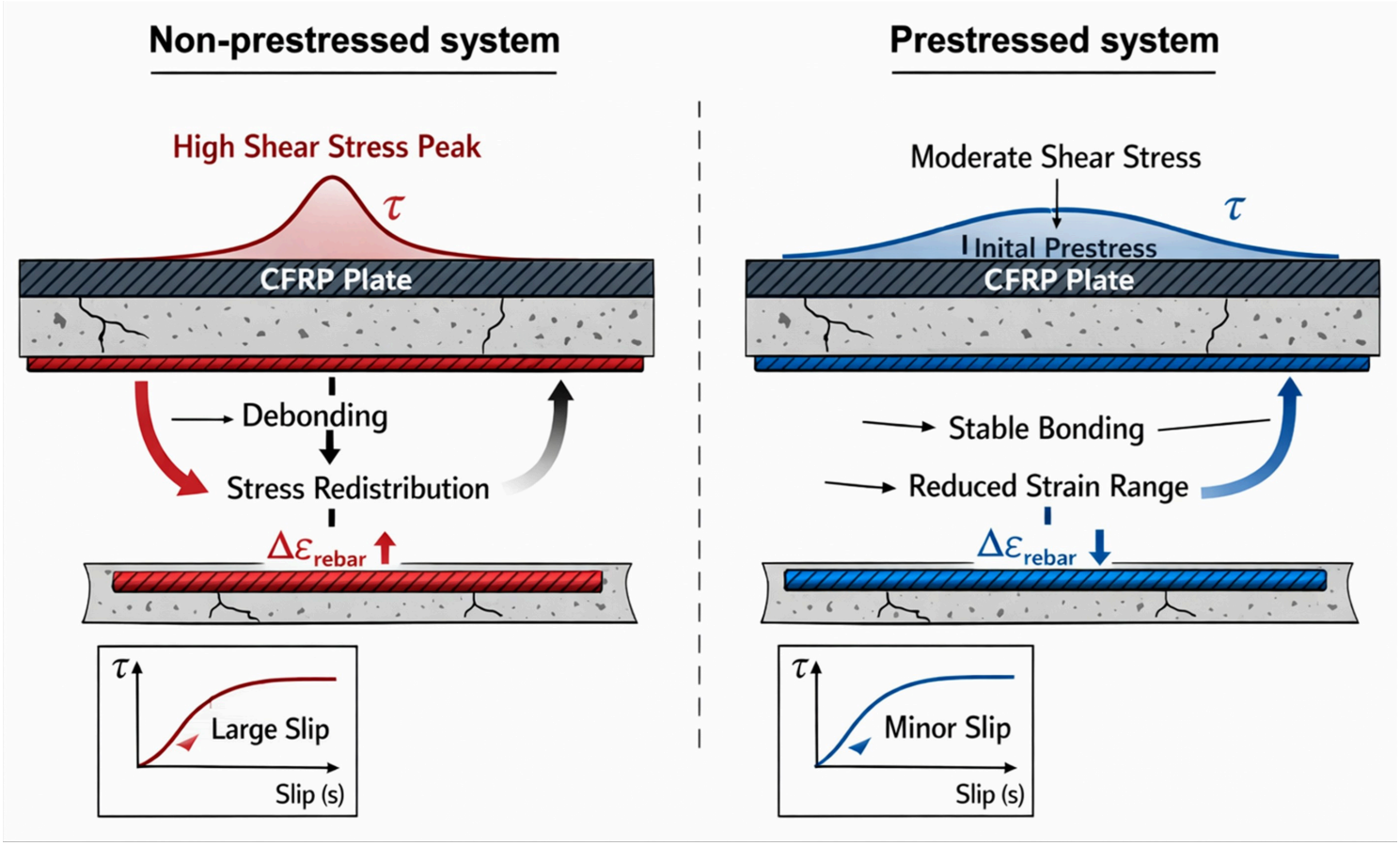


Figure 11

Illustration of fatigue damage evolution mechanisms in non-prestressed and prestressed CFRP strengthening systems

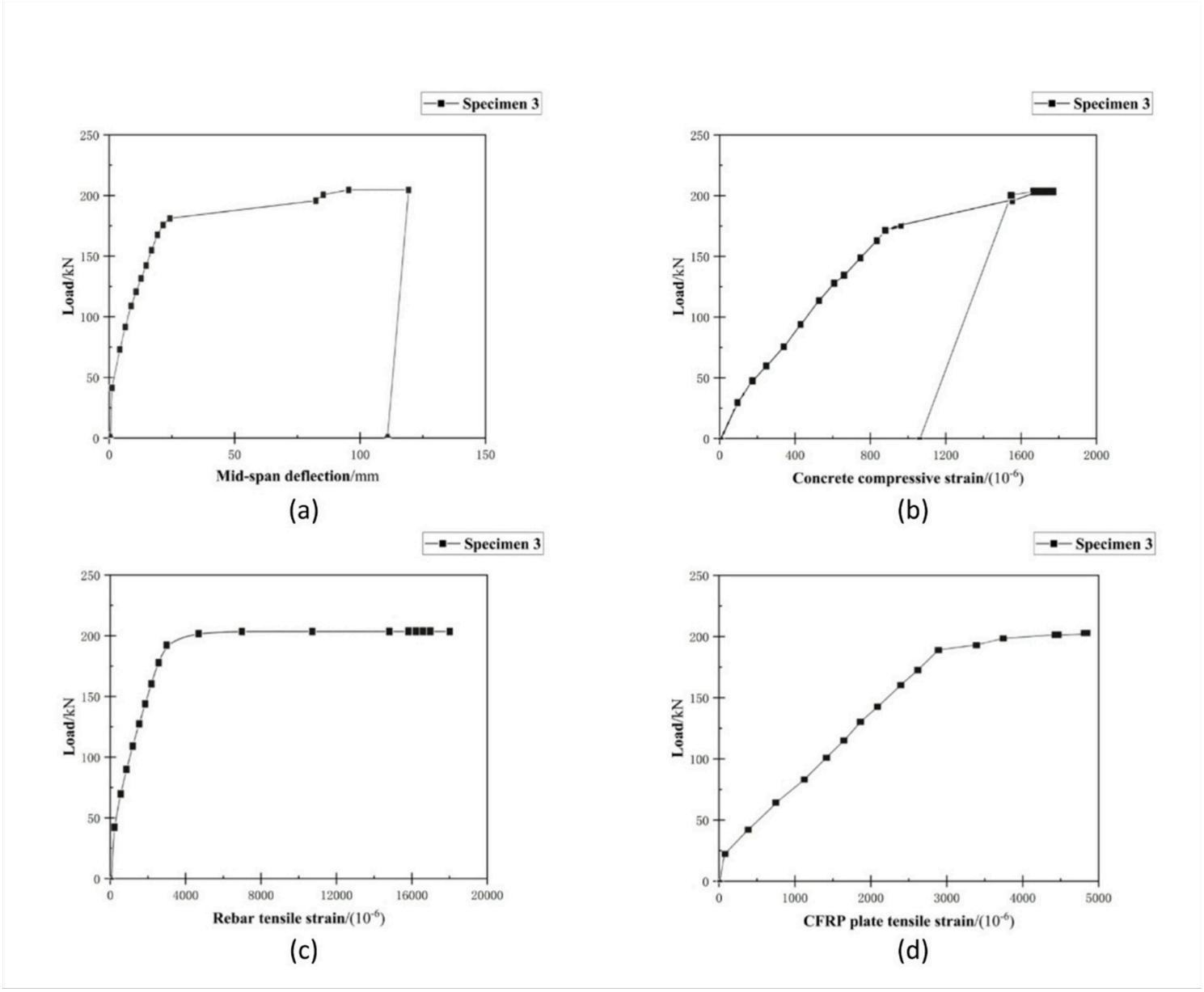


Figure 12

Variation of parameters during monotonic loading: (a) mid-span deflection, (b) concrete compressive strain, (c) rebar tensile strain and (d) CFRP plate strain

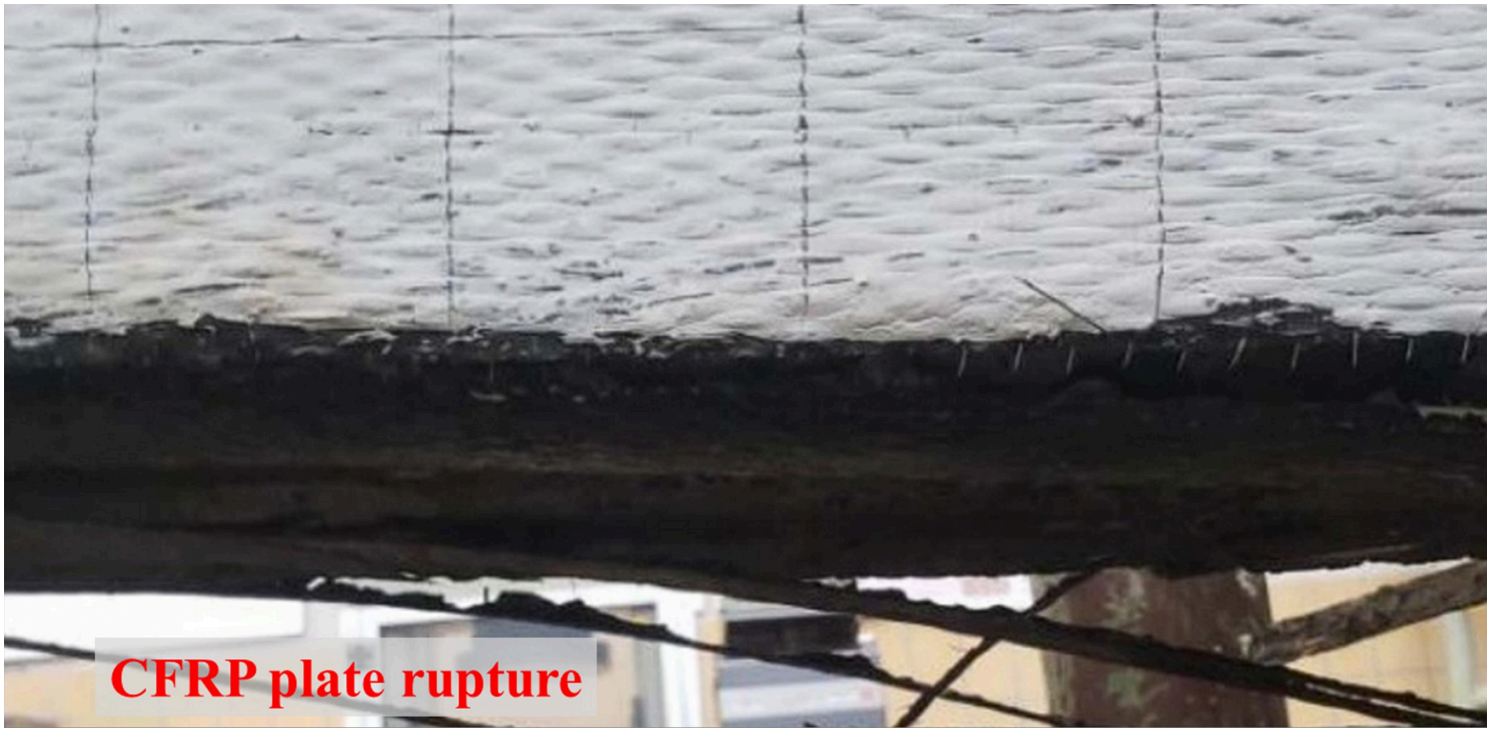


Figure 13

Flexural rupture of the CFRP plate